PROCEEDINGS OF SPIE

SPIEDigitalLibrary.org/conference-proceedings-of-spie

Optical processors for smart structures

Barry G. Grossman
Howard Hou
Ramzi H. Nassar

SPIE.

Optical processors for smart structures

Barry Grossman, Howard Hou, and Ramzi Nassar

Florida Institute of Technology, Department of Electrical Engineering
Optical Computing and Signal Processing Laboratory
150 West University Blvd., Melbourne, Florida 32901

ABSTRACT

For underwater fiber-optic sensor arrays containing hundreds of sensors as well as smart aerospace structures and skins using fiber-optic strain sensor arrays, the output of the sensors are optical signals that are a function of the measurand. We are also employing optical signals to energize smart-structure actuators (shape-memory alloys). An all-optical processor would thus seem to be the logical choice for the processor since we must simultaneously process, in real time, multiple optical input (sensor) signals and generate multiple output (actuator) signals. In addition, with an all-optical processor, there would be no reduction in processor performance due to converting between optical and electrical signals. We are developing hybrid optical processors[1] using an artificial neural network architecture to process the sensor inputs and calculate the resultant strain and optical control signals. This paper describes the computer simulations and experimental results performed to date. These results indicate that neural network architectures can successfully perform these very high-speed calculations with the desired accuracy. The current limitation in an all-optical implementation is in the performance of available bi-stable optical gate arrays.

1. INTRODUCTION AND GENERAL SYSTEM CONFIGURATION

Developments in material science have stimulated the development and use of composite materials in a wide range of applications,[2] including rotorcraft blades, advanced tactical fighter aircraft, ocean structures, and aerospace structures, such as the space station. Along with the advantages of an increased strength and stiffness-to-weight ratio, their use has raised a number of questions related to understanding the failure mechanisms involved, predicting failures far enough in advance to prevent them, and providing real-time structural strain (health) monitoring/damage assessment. Our method[3,4] for real-time strain monitoring uses fiber-optic sensors that can either be embedded into the composites or easily attached to the surface of existing composite or metallic structures.

Fiber-optic sensors can be embedded in composite materials during the manufacturing stage to monitor and control the process and, when used in conjunction with on-board fiber-optic data links, can then be used to monitor the health of the final assembled vehicle or platform. Embedded fiber-optic sensors can thus produce "smart structures" in which real-time sensing of structural conditions is accomplished by a distributed sensor system, which is an integral component of the structure. Processing the output from the sensors will allow real-time structural control when used with the appropriate actuators. Since fiber-optic sensors are sensitive along their total length, it is possible to determine, in real time, an indication of the structural integrity at all points along which the fiber runs, from centimeters to tens of kilometers.

A smart structure system is shown conceptually in Fig. 1. Optical fiber sensors monitor the desired spatial locations in the structure. The sensor outputs are connected to a processor,

which converts the changes in light output into time-varying spatial strain values. If the system is designed to react as well as sense, the processor will calculate the signals to be sent to embedded actuators, which subsequently modify the mechanical characteristics of the structure. In this way vibrations can be damped out or surface contours changed in addition to monitoring the structural integrity.

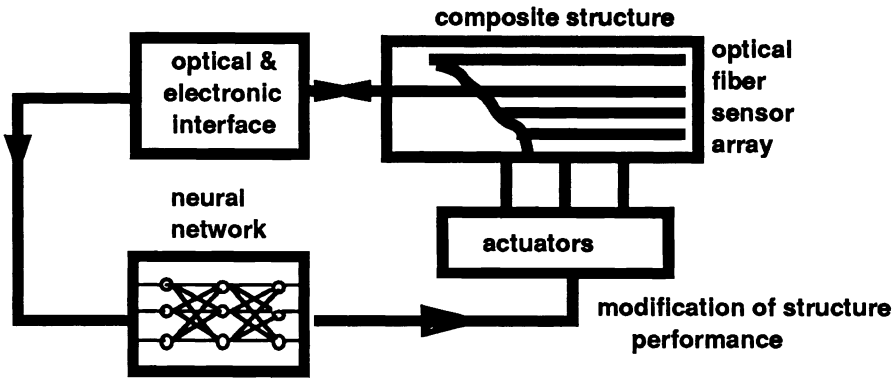

Figure 1. Block diagram of a smart structure system

Actuating device characteristics for smart structures are an important issue since levels of authority from the devices must be great enough to achieve performance goals, and the devices, when embedded in the structure, must be small enough so that structural integrity is not compromised. The actuating devices we are developing[5] are made from a shape-memory alloy (SMA). It undergoes a martensitic transformation in crystal structure when its temperature passes through a preset temperature transition point. In the process, it creates unusually large and usable forces. To heat the alloy through the transformation point, we illuminate it through an embedded optical fiber with a laser beam. Both the sensor output signal and the actuator control signal are optical. Using wavelength division multiplexing, it may be possible to use a single fiber both as a sensor and to illuminate multiple actuators.

The third major component of smart systems is the processor. For smart structures where sensing and actuation is distributed over large areas and consists of dozens to thousands of input and output elements, the task is computationally intensive and time consuming; sequential digital processors cannot provide the speed required. Artificial neural networks[6,7] offer a massive parallel architecture. The advantage of neural networks for an application like smart structures[8,9] lies both in its capability to analyze complex sensor signal patterns and in its speed in generating the appropriate control signals for the actuators. For three-layer perceptron networks, the processing speed is just three gate delays after off-line training, regardless of the number of inputs and outputs. This results in a total processing time that can be as small as a few tens of nanoseconds or less. The neural network learns the correct "algorithms" by example during training and is able to generalize to untrained inputs after training is completed. The inputs to the neural network are the fiber-optic sensor outputs, and the neural network outputs are the strain values and optical control signals for the actuators.

Neural nets have been primarily implemented using software simulation programs on conventional computers, but are now being developed in silicon parallel processing chips, optical systems, and hybrid electrooptic systems[10] that use electrooptic components with optical interconnects. Because the fiber-optic sensor inputs and the processor outputs to the actuators are both optical, a fully optical neural network computing system is the best

optical and electronic states. However, with practical, fully optical devices such as bi-stable gates and adaptive holographic interconnects still under development, a hybrid electrooptic system becomes attractive for the near term and also demonstrates the feasibility of an all-optical neural network for this application. We are developing a hybrid electrooptic system that demonstrates the feasibility of implementing an all optical neural network and that achieves the required performance.

2. NEURAL NETWORK ARCHITECTURES AND ALGORITHMS

Neural networks are processors that possess, to a very limited extent, some of the capabilities of the brain in learning, memorizing, and reacting. This means a capability to solve problems that are not easily defined algorithmically and to process parallel inputs in real time. Many different neural-network architectures have been studied[6,7] mathematically and implemented experimentally, primarily in software, including Hopfield, Kohonen, Boltzman machine, multilayer perceptron, etc. In our work, we have used the multilayer perceptron architecture shown in the figure below.

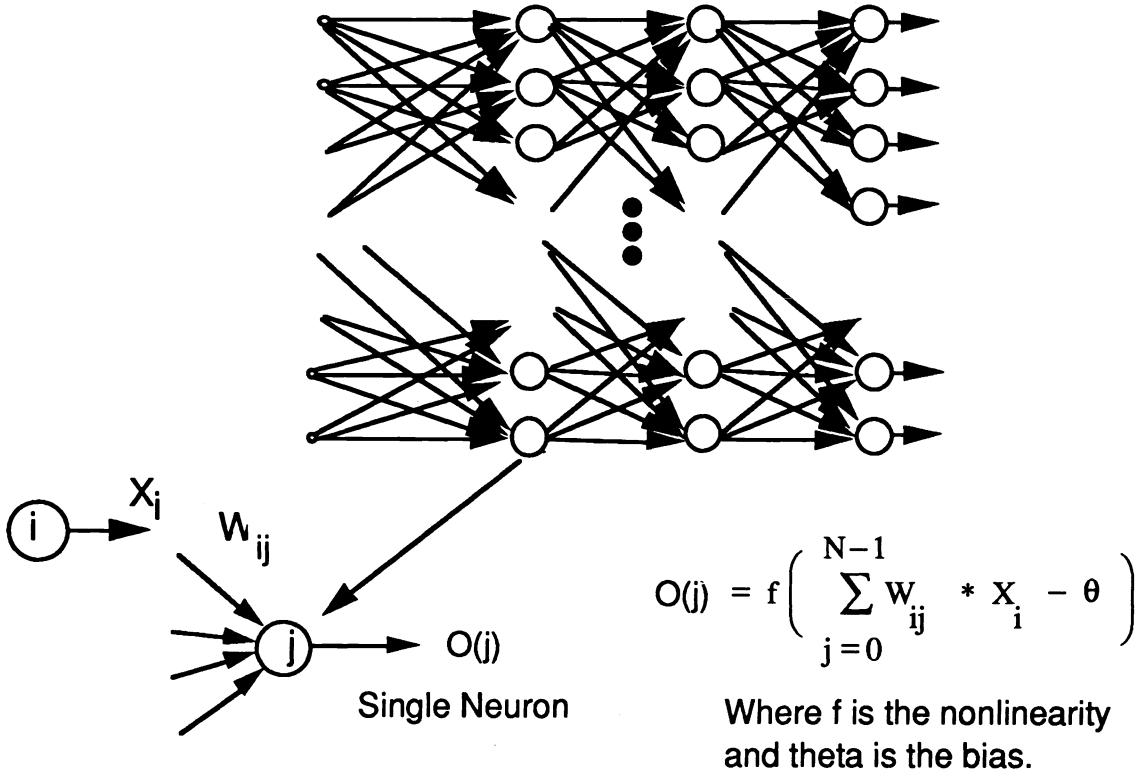

Figure 2. The training and use of artificial neural network processors for smart structures.

This architecture is a well-proven structure, and its use with back propagation for learning is a well-documented system. The multilayer perceptron training is based on back-propagation algorithms like that suggested in Lippman.[7] Outputs of each neuron are calculated from the equation

$$O(j) = f\left(\sum_{j=0}^{N-1} W_{ij} * X_i - \theta \right),$$

where W_{ij} is the weight from the ith to the jth node, X_i is the output of the ith node, θ is the bias, and f is the nonlinear function to be applied to the neuron. $O(j)$ is the output of the jth neuron.

The nonlinear activation function used was the sigmoid function given by

$$\text{f(inputs)} = \text{output} = 1/[1 + e^{-\text{sum(weighted inputs)}}]$$

The learning algorithm (back propagation) is calculated from either

$$W_{ij}(t+1) = W_{ij}(t) + \eta\delta_j X'_j$$

or with momentum alpha

$$W_{ij}(t+1) = W_{ij}(t) + \eta\delta_j X'_j + \alpha\left(W_{ij}(t) - W_{ij}(t-1)\right),$$

where with $d(j)$, the desired output is

$$\delta_j = O_j(1 - O_j)(d_j - O_j)$$

or for internal nodes,

$$\delta_j = X'_j\left(1 - X'_j\right)\sum_k \delta_k W_{jk}.$$

The network is trained by inputing sets of training values, letting the network calculate a set of outputs, and comparing the calculated and desired outputs. The error between them is used to modify the internodal weights using an appropriate learning algorithm. Another set of training data is then input to the network. This continues until the weight values converge to values that result in an output of sufficient accuracy for the complete set of training data. Once the network is trained, the weights are fixed, and it can be used to calculate the appropriate outputs with any similar input data, not only the training set.

3. NEURAL NETWORK SIMULATION RESULTS

3.1 Fiber-optic sensor training data

The fiber-optic strain sensor used[3,5] was a polarimetric sensor using low birefringence polarization preserving fiber. The sensor output as a function of strain is shown in Fig. 3.

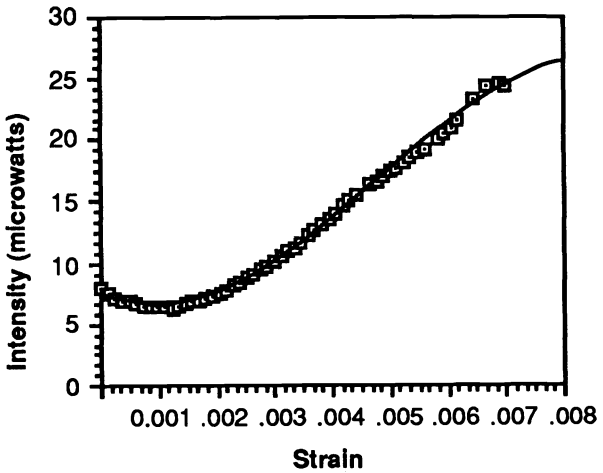

Figure 3. Strain sensor training data -Iout(strain)

3.2 Neural network simulation architecture and results

The architecture for the neural network used in the simulation is shown in Fig. 4.

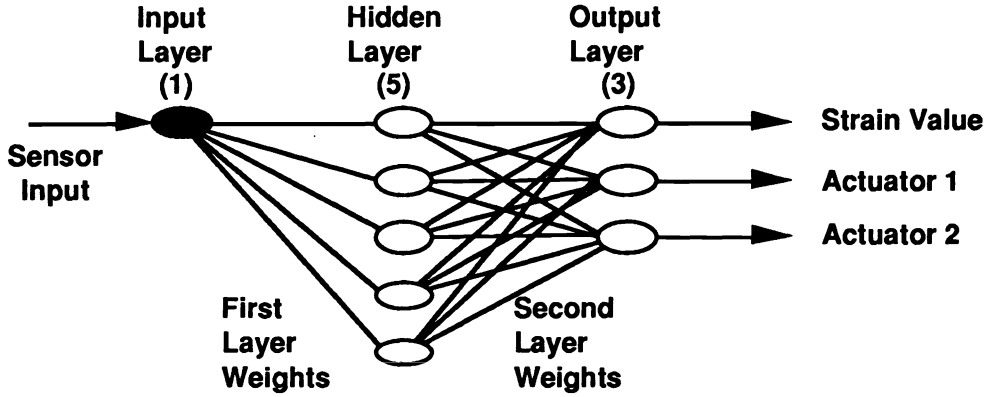

Figure 4. Neural network architecture used to calculate strain values from sensor output

The input is the sensor output light intensity corresponding to a particular strain value using the experimental data shown in Fig. 3. We varied the number of neurons in the hidden layer, searching for a compromise between accuracy of processing and using the minimum number of neurons. The results of the simulation performed on a VAX using our own software are shown in Fig. 5.

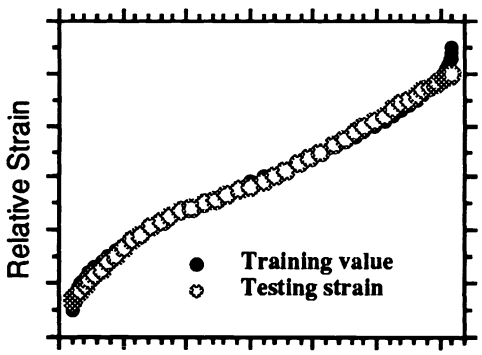

Figure 5.a Simulation results for 1/4/3 nodes RMS error/pattern = 2.82%.

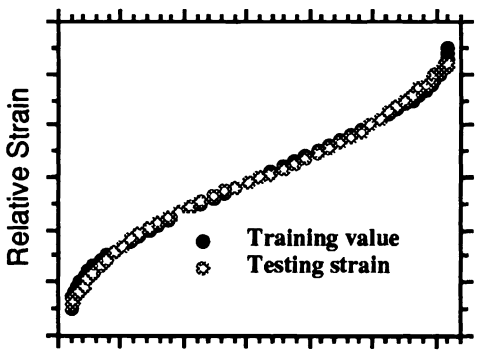

b. Simulation results for 1/60/3 nodes RMS error/pattern = 2.20%.

As shown in the two figures, the error obtained after training was very small (<2.5%) except at the two ends. The error at the ends, however, does not affect the system performance since it is outside the operation range of +/- 3000 microstrain. Since the difference in performance between the two cases is minimal, we decided to use the first configuration using four nodes in order to simplify the optical hardware implementation.

4. ELECTROOPTIC NEURON

The basic and most difficult element to implement is the neuron. It must function as an active device whose transfer function is the sigmoid function. Accuracy and response time are the two most important characteristics. As mentioned previously, we chose a hybrid approach discussed in the next section.

4.1 EO neuron block diagram

The block diagram of the EO neuron is shown below. The light input is the sum of weighted outputs from the previous layer. Part of the beam is split off and detected. It is this detected value that is digitized and input to the Apple II. There are 126 different pixel patterns stored in the computer, each corresponding to a different transmissivity value that can be input to the liquid crystal television (LCTV). The correct output pattern chosen has a transmissivity closest to that determined by the sigmoid function. Ideally the transfer function $T = I_{OUT}/I_{IN}$ of the optical part of the system is the desired sigmoid activation function, which is then weighted and input to the next layer.

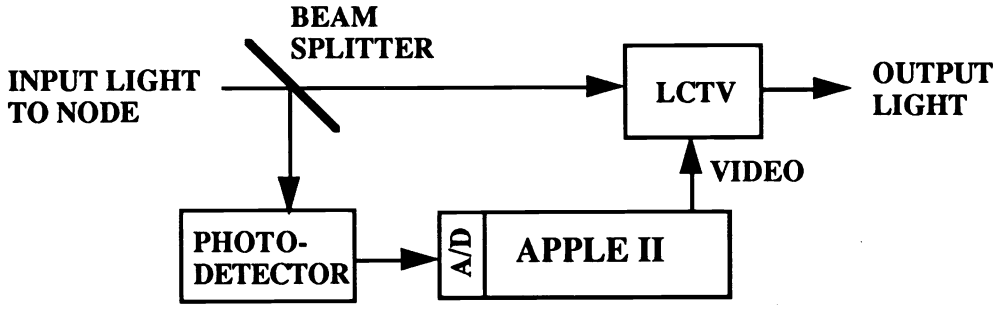

Figure 6. Block diagram of the EO neuron

4.2 Patterns/transmissivity values

The LCTV is the most critical device of the processor unit. To assure proper computations in real time, the performance of the LCTV was thoroughly investigated. Since a number of reports on the LCTV [1] have been published, we will concentrate here only on the neuron. Fig. 7 shows how we constructed the transfer function. The measured transmissivity values for every pixel pattern is shown on the graph on the right. The graph on the left shows the relation between net input intensity to one neuron and the output intensity obtained from the neuron. The slope in each equation is simply the transmissivity of a given pixel pattern, while the lines in the graph represent different transmissivities corresponding to pixel patterns from 1 to 126. By choosing the appropriate subset of the 126 pixel patterns, the sigmoid function (or any other) can be constructed.

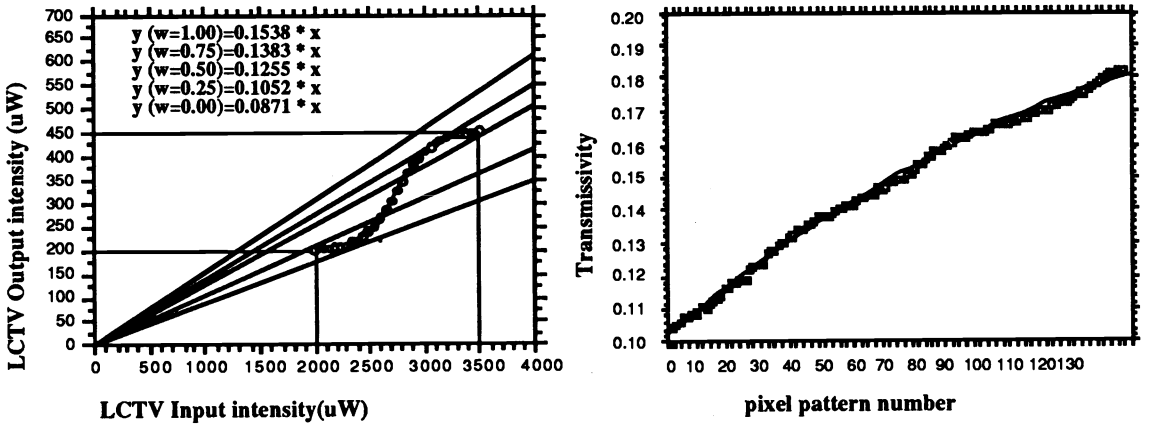

Figure 7. We can pick the correct set of pixel patterns to construct the sigmoidal output.

4.3 Static sigmoid values-theoretical vs experimental

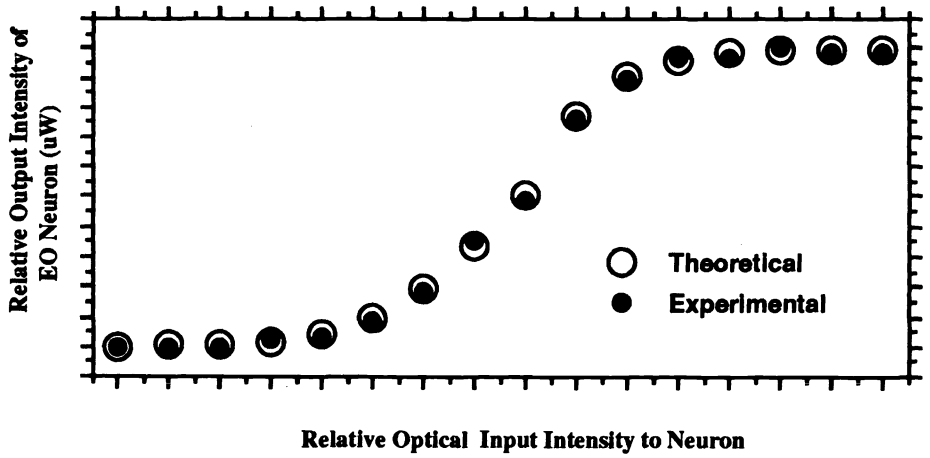

Figure 8. Exact vs static experimental measurement of neuron sigmoid response

The static measurements were made by varying the optical input, one point at a time, and measuring the optical output with an average-reading light meter once the computer/LCTV system reached its final value. The results are shown in Fig. 8. The agreement was excellent, with an average error of less than 2% over the complete output range. This small error is a result of the finite number of pixel patterns possible (due to the limited number of LCTV pixels).

4.4 Temporal response

The dynamic, or time/bandwidth, response of the neuron is limited primarily by the Apple computer processing time. This is the time required to take the input digital value (corresponding to the input light intensity), pick the stored pixel pattern corresponding to the sigmoid transfer function, and display it on the LCTV. The temporal optical output of the neuron was first measured using a low-frequency linear ramp function input. This should generate a repeating sigmoid function and is shown in Fig. 9 for two repetition rates, 3.0 Hz (left graph) and 0.3 Hz(right graph).

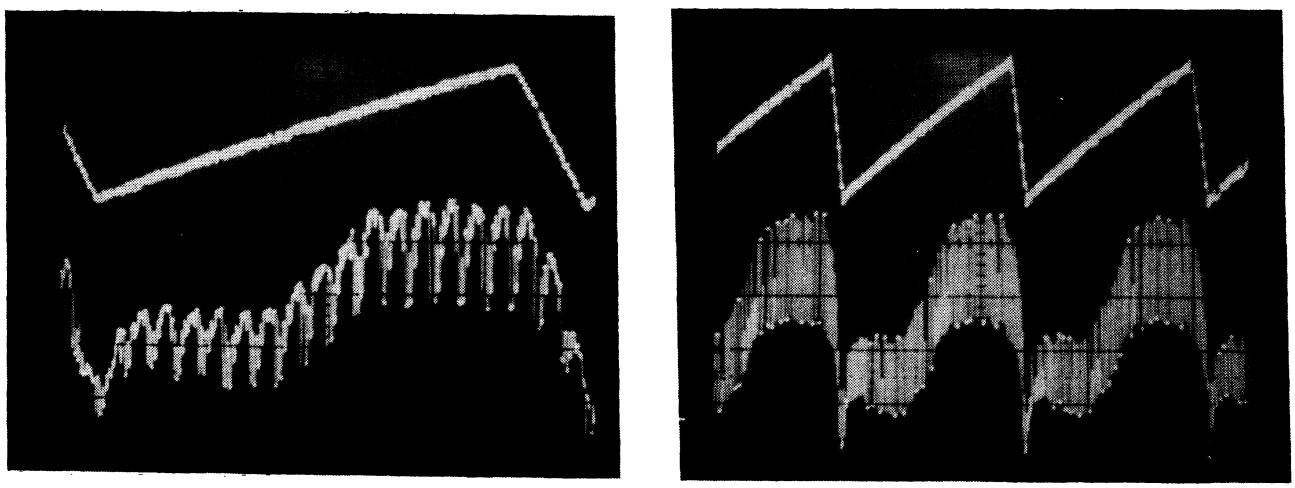

3 Hz ramp rate- 50 ms per division 0.3 Hz ramp rate- 1.0 second per division

Figure 9. Measured output light intensity with linear ramp input

As can be seen, a slowly varying linear input does produce the desired sigmoid optical output function. The sawtooth waveform inside the sigmoid envelope is the 60 Hz LCTV screen refresh rate. Thus the values measured in Fig. 8 are the sigmoid with the 60 Hz averaged out. For all practical purposes, the fastest neuron response is really limited by the LCTV to 16.6 msecond, the pixel refresh time.

We used a step input into the computer o determine the limiting time delay due to the computer system/LCTV. The computer must calculate a new pixel pattern and display it on the LCTV. Fig. 10 shows the typical response to a step change between one input value and another. There is a 500 ms delay (100 ms/div) between the step change and the onset of a change in the optical transmissivity due to the computer processing time. This is followed by a 16 ms rise time to the final output value. It is at this time that we write the new pixel pattern on the LCTV. The 500 ms computer delay, of course, directly depends on the speed of the processor, so some improvement could be obtained by using a faster processor.

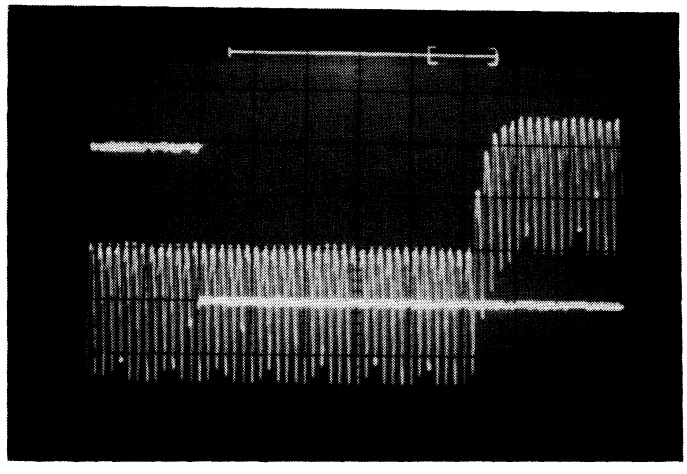

Figure 10. Typical output optical response to a step change between two input values

5. OPTICAL WEIGHTS

In addition to the neuron, optical weights must be implemented for the internodal interconnects. The Radio Shack LCTVs used here have, at their highest brightness setting, a 40% maximum transmission and a 9 % minimum transmission. When their contrast ratio is set to maximum, as was the situation on our system, the maximum transmission is reduced to 20%, as seen in Fig. 7. This is typical of this type of spatial light modulator and is the primary limiting factor to system dynamic range. To maximize the system throughput optical power, we generated fixed transparencies to implement the weighting functions instead of using LCTVs. We designed a number of different pixel patterns on the Macintosh, printed several transparencies on a laser printer, and measured the corresponding optical transmission for each pattern. Fig. 11 shows one of the transparencies, and the corresponding transmission of each individual patterns is shown in Fig. 12 a and b. Using the experimental results, we can pick the desired weight patterns to make the system weight masks. These will be the final trained weight values from the simulation.

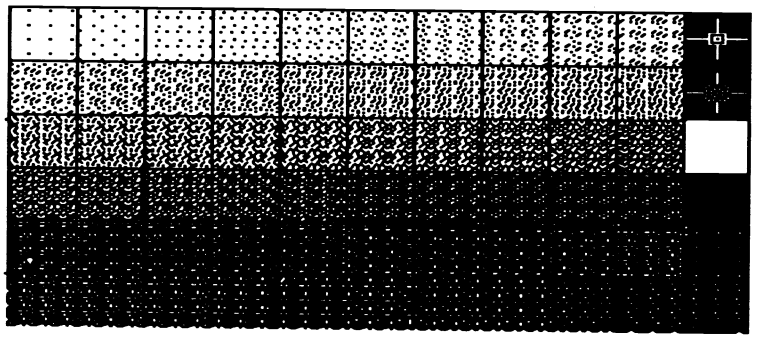

Figure 11. A transparency having 66 different patterns

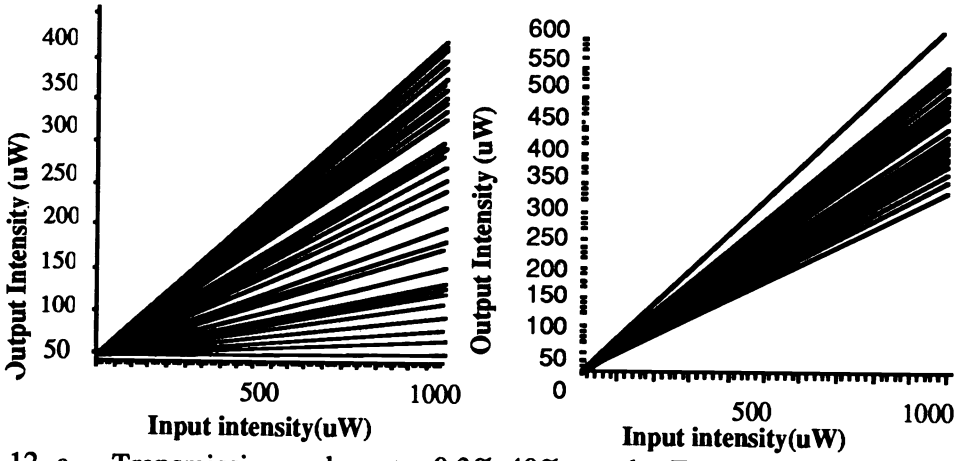

Figure 12 a. Transmission values to 0.3%-40% b. Transmission values 30%- 61%

Those values shown above are the transmission of each individual pattern on the transparency. The highest transmission obtained in this case was 61% and the lowest was 0.3%. Therefore, in our system, the final trained optical weights are limited within the range from 0.003 to 0.61. An important practical consideration is that the optical weight is an attenuation factor, which means the optical weight value has to be between 0 and 1.0 in all cases. However, in a practical system, there must also be a minimum output-signal-to-noise ratio, meaning that in certain configurations, the minimum transmission weight must be larger than zero. This places a severe constraint on allowable weight values.

6. NEURAL NETWORK ARCHITECTURE IMPLEMENTATION

We are currently implementing the neural network shown in Fig. 13. The optical system architecture being implemented is physically, but not architecturally, different from our simulation system shown in Fig. 4 . To reduce the optical system complexity, a combination of three equal networks with a 1x4x1 structure is being used instead. Each network will compute one output as indicated on the right side of the figure. The physical distribution on the LCTV's screen is shown on the left side of the figure. Although the LCTV displays every neuron on the screen at the same time, two LCTVs are still required to implement the system because a two layer neural network cannot compute its input and output layers at the same time.

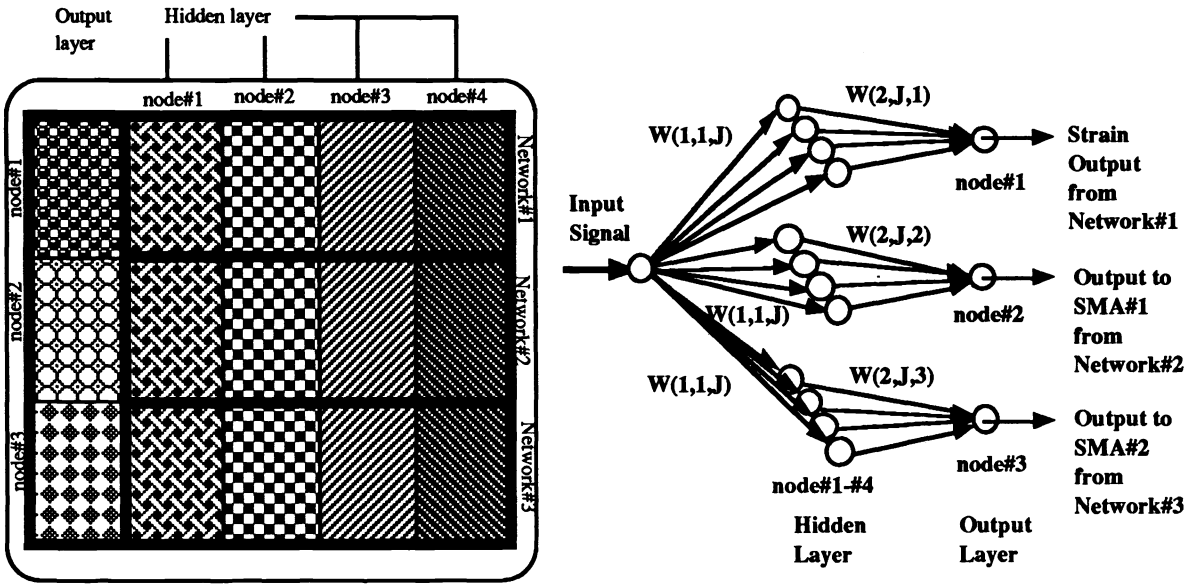

Figure 13. Neural network system architecture implemented/distribution of neurons on the LCTV's screen.

As discussed above, the LCTV system will implement the EO neurons. Fixed transparency weight masks will be used for the inter-neural weights, and an anomorphic imaging system will provide the optical interconnections. Clocking signals will be generated for each layer to allow each layer of neurons to produce the proper output before the next layer calculates its output. Once the system is finished we will compare its performance to the desired and simulated output values. We also plan to investigate the effects of optical crosstalk and limited weight accuracy on the results.

7. CONCLUSIONS

We have successfully demonstrated and characterized an electrooptic neuron capable of being utilized as a basic building block of an artificial neural network for processing fiber-optic sensor signals. The neuron transfer function is the desired sigmoid function, accurate to within 2%. Its dynamic response is limited to 500 milliseconds by the computer (1 MHz clock) used in our system. This can easily be reduced to 50 milliseconds using a different processor running at a higher speed. The real limiting factor is the screen refresh rate of the LCTV, 16.7 milliseconds.

We have also designed and performed computer simulations of an EO neural network system of seven nodes. The simulation predicts a processing accuracy of better than 2.5% in calculating the strain corresponding to any fiber-optic sensor signal output level. The accuracy is within this bound over the sensor range of +/- 3000 microstrain. We are currently building the complete system, which we will demonstrate and characterize.

8. ACKNOWLEDGMENTS

The authors would like to acknowledge the helpful suggestions of Dr. Mike Thursby and the assembly language development performed by Mr. Ya-di Lin and Mr. Bard. The work was performed in the Optical Computing and Signal Processing Laboratory at Florida Institute of Technology.

9. REFERENCES

1. B. Grossman, H. Hou, and R. Nassar, "Electrooptic Neural Processors for Smart Sensors and Structures," invited paper, IEEE Southcon '90, proceedings, Orlando, Fla.

2. B. Grossman and M. Thursby, "Embedded Sensors for Smart Structures," invited paper, American Institute of Aeronautics and Astronautics Technical Symposium on Spaceport Operations and Technology, Cocoa Beach, Fla., February 1989.

3. T. Alavie, B. Grossman, and M. Thursby, "Processing of One Fiber Interferometric Sensor Signals," SPIE OE/FIBERS 1989, conference and proceedings, Boston, Mass., September 1989.

4. B. Grossman, M. Thursby, and T. Alavie, "Modeling, Acquisition, and Processing of Embedded Fiber-optic Strain Sensor Signals," AMSE International Signals and Systems Conference, Miami, Fla., March 1989.

5. B. Grossman, T. Alavie, F. Ham, J. Franke, and M. Thursby, "Fiber-optic Sensors and Smart Structures Research at Florida Institute of Technology," SPIE OE/FIBERS 1989, conference and proceedings, Boston, Mass., September 1989.

6. M. Caudill, "Neural Networks Primer," *AI Expert*, December 1987.

7. R. Lippmann, "An Introduction to Computing with Neural Nets," *IEEE ASSP Magazine*, April 1987.

8. B. Grossman, F. Ham, M. Thursby, and T. Alavie,"Use of Artificial Neural Processors and Fiber-optic Sensors for Control of Smart Structures," ASME Annual Meeting, Adaptive Structures Session, San Francisco, Calif., December 1989.

9. M. Thursby, B. Grossman, T. Alavie, and K. Yoo, "Smart Structures Incorporating Artificial Neural Networks, Fiber Optic Sensors, and Solid State Actuators," SPIE OE/FIBERS 1989, conference and proceedings, Boston, Mass, September 1989.

10. N. Farhat, "Optoelectronic Neural Networks and Learning Machines," *IEEE Circuits and Devices Magazine*, Vol. 5, No. 5, September 1989.